Optics Letters

Determination of the refractive-index change in the excited state based on transient absorption microscopy

Tianyu Huo, Lihe Yan,* Jinhai Si, Peipei Ma, Yanan Shen, and Xun Hou

Key Laboratory for Physical Electronics and Devices of the Ministry of Education & Shaanxi Key Laboratory of Photonics Technology for Information, School of Electronic Science and Engineering, Xi'an Jiaotong University, No. 28, Xianning West Road, Xi'an 710049, China
**liheyan@mail.xjtu.edu.cn*

Received 15 September 2023; revised 8 November 2023; accepted 15 November 2023; posted 16 November 2023; published 13 December 2023

Photoinduced excited-state carriers can affect both the absorption coefficient and refractive index of materials and influence the performance of photoelectric devices. Femtosecond time-resolved pump–probe transient absorption (TA) spectroscopy is usually used to detect carrier dynamics and excited-state absorption coefficients; however, measurements of transient refractive-index change are still difficult. We propose a method for determining the excited-state refractive-index change using TA microscopy. In TA measurements, a Fabry–Pérot cavity formed by the front and back surfaces of the sample could lead to interference of the probe light. As the wavelength of standing waves in the Fabry–Pérot cavity is closely related to the refractive index, the carrier-induced excited-state refractive-index change was obtained by comparing the transmission probe spectra between the ground and excited states. The proposed method was used to study the dynamics of excited-state refractive-index change in a perovskite film.

https://doi.org/10.1364/OL.506090

Photoinduced carriers play an important role in the opto-electric responses of materials and devices. These charge carriers in the excited state undergo various ultrafast relaxation processes, such as dissociation, transport, and recombination [1,2], and also produce transient changes in the absorption coefficient and refractive index of the excited material [3,4]. The modulation of these optical parameters can influence the photoelectric response of materials in multiple ways. For example, excited state absorption (ESA), which has been studied extensively in organic solar cells and nonlinear optical devices, can affect the photoelectric conversion and optical nonlinearity of organic molecules [5–7]. Our latest studies proved that changes in the refractive index of a material in the excited state affected the temporal and spectral characteristics of a microcavity laser [8]. Therefore, to clarify the dynamics of photoinduced carriers and their effects on the photoelectric response of materials, transient changes in the absorption coefficient and refractive index of materials in the excited state must be determined.

Generally, the change in optical parameters is of the order of one-thousandth or even lower when materials are pumped to the excited state. Femtosecond time-resolved transient absorption spectroscopy (fs-TAS) [9,10] is widely used to measure the change in the absorption coefficient of materials. Although the absorption cross section of the excited state can be easily obtained, the change in the refractive index in the excited state is hard to be determined directly. To measure the refractive-index changes, Tamming *et al.* referred to Michelson interferometer and introduced a reference pulse in the TA setup [11]. The interference between the probe and reference pulses was used to analyze the refractive-index change. However, the time interval between two pulses could limit the timescale of the dynamic measurement. Pasanen *et al.* derived an equation to calculate the refractive-index change [12] from the transient transmittance, transient reflection, and steady-state transmittance/reflectance spectra, and thereby complex measurements and calculations limited the application of the method. In fs-TAS measurements, if the sample has clean and smooth surfaces, the self-assembled Fabry–Pérot (F–P) cavity can be formed, leading to interference of the probe light. In this situation, the pump-induced refractive-index change affects the frequency spacing between two standing waves formed in the resonator, which is known as the free spectral range (FSR). Therefore, the transient refractive-index change of the medium can be obtained by comparing the transmission spectra of the probe light with different FSR in the ground (without pump light excitation) and excited (with pump light excitation) states. Moreover, due to the wide spectral range of the probe light, more interference cycles can be obtained providing convenience for analysis.

In traditional TAS measurements, laser beams are focused on a sample using a lens, and the spot size is typically tens of microns. Within the irradiation region, the roughness and nonuniformity of the sample surface may eliminate the interference effect. By combining TAS and microscopy [13–15], the laser beams are focused using an objective lens, and TA spectra can be obtained from a region of interest with a size of microns or even smaller. In such a small area, surfaces of the sample tend to be more uniform, and the interference of the light reflected by the front and back surfaces can easily occur. Consequently, the transient refractive index of the excited state can be determined.

In this study, we explored the change in the refractive index in the excited state based on the proposed method by using a home-built transient absorption microscopy (TAM) system.

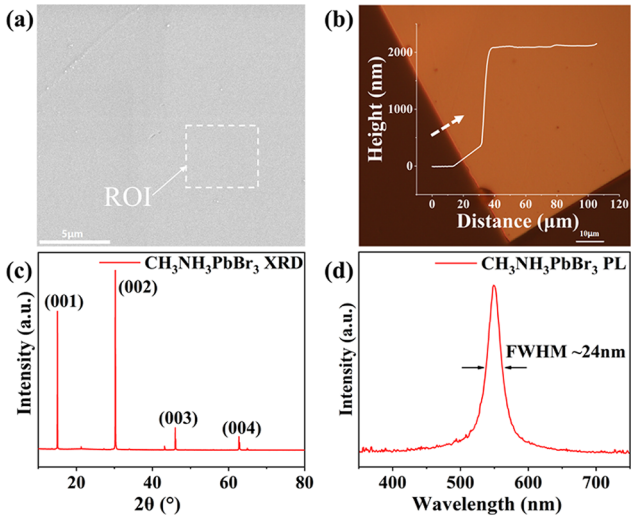

Fig. 1. Characterization results of the sample. (a) SEM image. (b) Optical microscope image and sample thickness measured by a step profiler. (c) Results of XRD characterization. (d) PL spectra.

$CH_3NH_3PbBr_3$ single-crystal perovskite thin films prepared by the space-limited method were excited by a 400 nm femtosecond laser pulse with different pump fluences and detected by a white light supercontinuum used as a probe. The obtained TA spectra were decorated with a series of striped patterns. By establishing a model related to the transient change in the refractive index, the dynamics of the refractive-index change in the excited state were successfully extracted from fitting results. The origin of striped patterns was revealed and attributed to a relative change in the interference spectra when the sample was in the excited and ground states. This study demonstrated the possibility of using the TA spectra to study carrier-induced, small changes in the refractive index. These findings may be a useful reference when using TAM technology, and the experimental method could serve as a novel approach for studying the refractive index of samples in the excited state.

We fabricated high-quality $CH_3NH_3PbBr_3$ single-crystal perovskite films using the space-limited preparation method [16]. First, the morphology, crystal structure, and chemical properties of single-crystal films were characterized (Fig. 1). Figure 1(a) shows a scanning electron microscopy (SEM) image. Benefiting from slow crystallization assisted by the anti-solvent diffusion process of the space-limited method, the film exhibits the characteristics of large size (several tens of microns), good flatness, and a clean surface. The white dashed box indicating the region of interest (ROI). Figure 1(b) shows the morphology observed under an optical microscope. Using a step profiler along the direction of the dashed arrow, the sample thickness was estimated to be approximately 2.1 μm. The crystal lattice structure was characterized by x ray diffraction (XRD), as shown in Fig. 1(c). The sharp peaks of 2θ at 15.04°, 30.22°, 45.98°, and 62.72° correspond to the (001), (002), (003), and (004) crystal faces of cubic phase $CH_3NH_3PbBr_3$, which is consistent with previous reports [17,18]. The narrow full width at half maximum (FWHM) of each peak indicates that the sample has good single-crystal properties. The photoluminescence (PL) spectra with a central wavelength of 549 nm and FWHM of approximately 24 nm were acquired using a frequency-doubled 400 nm pulse laser as the excitation light [19], as shown in Fig. 1(d).

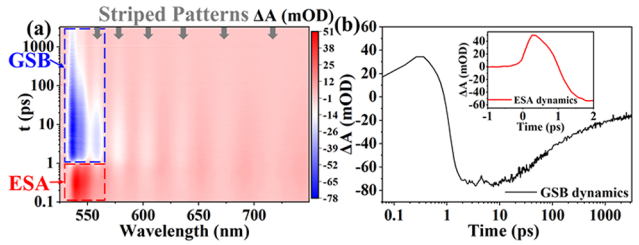

Fig. 2. (a) 2D pseudo-color diagram of TA spectra with striped patterns. (b) GSB dynamics and ESA dynamics (inset).

Subsequently, fs-TAM measurements were conducted on the $CH_3NH_3PbBr_3$ single-crystal perovskite thin films. Figure 2(a) shows a two-dimensional (2D) pseudo-color diagram of the acquired TA spectra. There are three obvious TA signals: negative signal (blue dashed box), positive signal (red dashed box), and striped patterns (gray arrows) between approximately 560–750 nm. The peak wavelength of the negative signal is close to the bandgap of $CH_3NH_3PbBr_3$. This is generally referred as the ground state bleaching (GSB) signal and originates from the band-filling effect [20,21]. Electrons occupy the conduction band by absorbing photons and weaken the further absorption. Therefore, a negative transient change in the absorption coefficient would be observed. Compared with the negative signal, the positive signal is located at the redshifted position and lasts for an extremely short time. This is a widely researched ESA phenomenon in semiconductors, which is induced by the bandgap renormalization effect [22,23]. Photons with energy larger than the bandgap induce hot carriers, leading to the shrink of the band edge. The new transition between the modified band-edge states corresponds to absorption enhancement and behaves as a positive signal. These two signals are typical signatures of TA spectra and are typically used to analyze the ultrafast dynamics of carriers at the bottom of the conduction band and hot carriers [24–26]. Figure 2(b) shows the dynamics of GSB signal and ESA signal. Due to the overlap of the two signals, the sign of the GSB signal in short delay time is positive and the sign of ESA signal gradually becomes negative. Through global fitting analysis [24], the influence of wavelength overlap can be removed, and the real process can be extracted. However, it is important to note that a series of striped patterns occurred in the long-wavelength direction, which is rarely observed in the TA spectra.

To clarify the origin of striped patterns, we investigated the TA spectra for different delay times, as shown in Fig. 3(a). The striped patterns in the 2D pseudo-color diagram behaved as wave-like curves in the TA spectra at a certain delay time. For the convenience of independently studying the striped patterns, the GSB signal was subtracted from the TA spectra to obtain curves with only striped characteristics; the corresponding results are shown in Fig. 3(b). The contrast of striped patterns gradually decreases with increasing delay time, displaying the same trend as the GSB signal. The weakening of the GSB signal intensity implies the recombination of electrons in the conduction band with holes in the valence band and reduction in carrier concentration. Therefore, striped patterns were also influenced by carriers in the excited state.

In addition to striped patterns in the TA spectra, a wave-like curve was observed in the steady-state transmission spectra. As our sample had smooth surfaces and the studied region was extremely small, the front and back surfaces could form an F-P

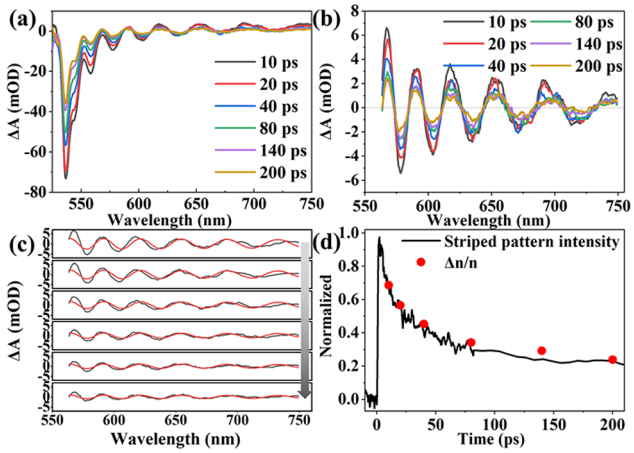

Fig. 3. (a) TA spectra at different delay times. (b) TA spectra with only the striped characteristics after subtracting the GSB baseline. (c) Fitting results (red lines) of striped patterns (black lines) through the proposed model. The direction of gray arrow indicating the increase of delay time. (d) Change in refractive index extracted from the fitting (red dots) and the contrast of the stripe valley at 603 nm (black line) as a function of the delay time.

cavity structure, resulting in interference. Constructive interference will occur when $2nd$ equals to $k\lambda$, where n, d, and k are the refractive index, the sample thickness, and an integer, respectively. After the carriers in the excited state were injected by pump light, the refractive index was modified, and the degree of interference was enhanced or weakened for light with different wavelengths. When the sample is in the ground state and possesses an intrinsic refractive index n, the intensity of light with wavelength λ passing through it can be defined as $I_{(\lambda,\text{ground})}$. After the sample is pumped to the excited state and the refractive index changes to $n-\Delta n$, the transmission intensity correspondingly changes to $I_{(\lambda,\text{excited})}$. According to the calculation method for the TA signal $\Delta OD = log_{10}^{(I_{(\lambda,\text{ground})}/I_{(\lambda,\text{excited})})}$, ΔOD will be nonzero if the refractive index changes. Owing to a wide spectral range of the probe light used in our experiments and the wavelength dependence of the degree of interference, the difference in the transmission spectra between the excited and ground states manifested as a wave-like curve when interference occurred.

Based on the above description, the decrease in the intensity of striped patterns could be attributed to a reduction in the carrier concentration. During the relaxation of carriers, the sample gradually returned to the ground state and the carrier-induced refractive-index change Δn gradually changed to zero. Finally, the transmission spectra will remain constant, and striped patterns will no longer be present in TA spectra. To further reveal the relationship between the interference and TA spectra, a model for the transient refractive-index change was created, as shown below. In this model, I_0 represents the incident light intensity, while I_1 and I_2 are the reflected light intensities of the front and back surfaces of the sample, respectively. They can be calculated using $I_1 = I_0 \cdot R$ and $I_2 = (I_0 - I_1) \cdot R$, respectively, where R is the reflectivity. The intrinsic refractive index of the sample and the change in the refractive index caused by photoinduced carriers are represented by n and Δn, respectively. Thus, the refractive index of the sample in the excited state is $n' = n - \Delta n$. The expression in the outer parentheses of the numerator represents

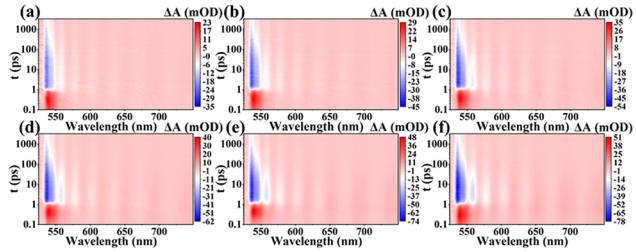

Fig. 4. 2D pseudo-color diagram of TA spectra with striped characteristics under different pump fluences: (a) 46.7 μJ/cm^2, (b) 54.1 μJ/cm^2, (c) 61.4 μJ/cm^2, (d) 70.1 μJ/cm^2, (e) 82.3 μJ/cm^2, and (f) 99.5 μJ/cm^2

the calculation of coherent interference intensity between lights reflected by the front and back surfaces. Accordingly, the entire numerator represents the transmission intensity after interference, while the denominator corresponds to the situation in which the sample is in the excited state. Therefore, the overall form of the formula is a combination of the TA calculation principle and the interference principle. Finally, the TA signal intensity in ΔOD units can be calculated:

$$\Delta OD = log_{10}\frac{I_0 - \left(I_1 + I_2 + 2\cdot\sqrt{I_1\cdot I_2}\cdot\cos\left(\frac{4\pi nd}{\lambda}\right)\right)}{I_0 - \left(I_1 + I_2 + 2\cdot\sqrt{I_1\cdot I_2}\cdot\cos\left(\frac{4\pi n'd}{\lambda}\right)\right)}.$$

The striped patterns were fitted using this model, and results are shown in Fig. 3(c). This was used to obtain the intrinsic refractive index n of approximately 2.6 and the change in the refractive index Δn at each delay time. Consistent with the above analysis that refractive-index change would gradually decrease to zero, $\Delta n/n$ decreases from 13.5×10^{-4} at 10 ps delay time to 4.69×10^{-4} at 200 ps delay time. The dynamics of the stripe signal intensity and $\Delta n/n$ are compared in Fig. 3(d). The black line represents the normalized dynamic process of the signal intensity at 603 nm, which is the third valley of the striped patterns and away enough from the GSB signal range, while the red dots represent the normalized $\Delta n/n$ obtained by fitting. They were consistent with each other, further validating that striped patterns are induced by the change in the refractive index and the reliability of the proposed model.

Because the initial photoinduced carrier concentration is related to the number of absorbed photons, we further investigated this phenomenon under various pump fluences. The 2D pseudo-color diagrams of the TA spectra under each pump fluence are shown in Fig. 4, which displays clear striped patterns. Furthermore, the TA spectra at the same delay time (10 ps) were extracted and compared, as shown in Fig. 5(a). The evolution of the GSB signal intensity and striped pattern intensity shares the same trend with decreasing pump fluence. As explained previously, the change in the refractive index decreased with the carrier concentration, leading to a decrease in the difference in the transmission spectra between the excited and ground states. To ensure that the injected carrier concentration was proportional to the pump fluence, pump fluences used in our experiments were maintained at a low level. We compare the peak intensity of the GSB signal as a function of the pump fluence in Fig. 5(d), as indicated by the red dotted line. The linear relationship between them indicates that the sample exhibits a linear absorption of the pump light within the applied fluences. After subtracting the GSB signal baseline, the acquired curves with only striped characteristics are shown in Fig. 5(b), and the

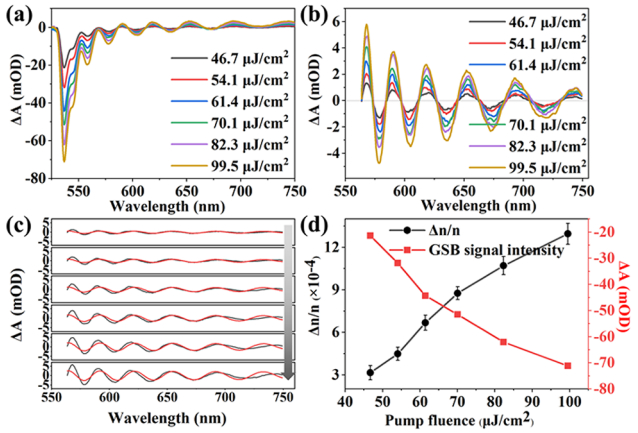

Fig. 5. (a) TA spectra under different pump fluences at 10 ps delay time. (b) TA spectra with only the striped patterns after subtracting the GSB baseline. (c) Fitting results (red lines) of striped patterns (black lines) through the proposed model. The direction of gray arrow indicating the increase of pump fluence. (d) Change in the refractive index extracted from fitting results (black line) and peak intensity of the GSB signal (red line) as a function of the pump fluence.

fitting result for this dataset is shown in Fig. 5(c). The extracted intrinsic refractive index is approximately 2.6, which is consistent with previous experimental results. From the fitting result, the change rate of the refractive index $\Delta n/n$ is plotted in Fig. 5(d) as a function of the pump fluence. It should be noted that due to the overlap of wavelength range between the GSB signal and striped patterns, the short wavelength of striped patterns will still be affected after subtracting the GSB baseline, thus reducing the fitting accuracy at short wavelength direction. Under pump fluences of 46.7 μJ/cm^2 and 99.5 μJ/cm^2, the values of $\Delta n/n$ are 3.15×10^{-4} and 12.9×10^{-4}, respectively. Notably, $\Delta n/n$ varies linearly with the carrier concentration, which is consistent with previous reports. Pump–fluence-dependent experiments further support this explanation.

In summary, we used a home-built TAM setup to conduct detailed studies on the change in the refractive index induced by carriers. The physical origin of striped patterns appearing in the TA spectra was clarified and attributed to the contribution of the refractive-index change induced by the change in carrier concentration between the excited and ground states. The experimental data with striped pattern characteristics were fitted using an established model related to the refractive index. The fitting results provided information regarding the refractive index in the excited state as a function of the delay time and pump fluence. Our work demonstrates the possibility of using TAM to investigate dynamic changes in the refractive index in the excited state. The experimental findings may aid in understanding the special phenomena that may occur when using TAM to study thin-film samples. Furthermore, this technique can serve as a unique approach for studying refractive index of a sample in excited state.

Funding. National Natural Science Foundation of China (62027822); National R&D Program of China (2019YFA0706402).

Acknowledgment. L. H. Y. and T. Y. H. conceived the study. T. Y. H. and Y. N. S. designed the system and performed the experiments. P. P. M. prepared the samples. L. H. Y. and T. Y. H. discussed the results, analyzed the experimental data, and wrote the manuscript. All authors were involved in revising the manuscript.

Disclosures. The authors declare no conflicts of interest.

Data availability. The data underlying the results presented in this paper are not publicly available at this time but may be obtained from the authors upon reasonable request.

REFERENCES

1. C. S. Ponseca Jr, P. Chabera, J. Uhlig, *et al.*, Chem. Rev. **117**, 10940 (2017).
2. C. Jin, E. Y. Ma, O. Karni, *et al.*, Nat. Nanotechnol. **13**, 994 (2018).
3. J. G. Mendoza-Alvarez, F. D. Nunes, and N. B. Patel, J. Appl. Phys. **51**, 4365 (1980).
4. B. R. Bennett, R. A. Soref, and J. A. Del Alamo, IEEE J. Quantum Electron. **26**, 113 (1990).
5. T. Trupke, M. A. Green, and P. Würfel, J. Appl. Phys. **92**, 4117 (2002).
6. Y. Li, L. Yan, J. Si, *et al.*, J. Chem. Phys. **156**, 054702 (2022).
7. D. C. Rodenberger, J. R. Heflin, and A. F. Garrto, Nature **359**, 309 (1992).
8. P. Ma, L. Yan, J. Si, *et al.*, Laser Photonics Rev. **11**, 2300533 (2023).
9. R. Berera, R. van Grondelle, and J. T. Kennis, Photosynth. Res. **101**, 105 (2009).
10. C. Ruckebusch, M. Sliwa, P. Pernot, *et al.*, J. Photochem. Photobiol., C **13**, 1 (2012).
11. R. R. Tamming, J. Butkus, M. B. Price, *et al.*, ACS Photonics **6**, 345 (2019).
12. H. P. Pasanen, P. Vivo, L. Canil, *et al.*, Phys. Chem. Chem. Phys. **21**, 14663 (2019).
13. M. C. Fischer, J. W. Wilson, F. E. Robles, *et al.*, Rev. Sci. Instrum. **87**, 031101 (2016).
14. D. Y. Davydova, A. de la Cadena, D. Akimov, *et al.*, Laser Photonics Rev. **10**, 62 (2016).
15. Y. Zhu and J. X. Cheng, J. Chem. Phys. **152**, 020901 (2020).
16. Z. Yang, Q. Xu, X. Wang, *et al.*, Adv. Mater. **30**, 1802110 (2018).
17. H. Di, W. Jiang, H. Sun, *et al.*, ACS Omega **5**, 23111 (2020).
18. W. Peng, L. Wang, B. Murali, *et al.*, Adv. Mater. **28**, 3383 (2016).
19. D. Shi, V. Adinolfi, R. Comin, *et al.*, Science **347**, 519 (2015).
20. N. Mondal and A. Samanta, Nanoscale **9**, 1878 (2017).
21. J. S. Manser and P. V. Kamat, Nat. Photonics **8**, 737 (2014).
22. G. Trankle, E. Lach, A. Forchel, *et al.*, Phys. Rev. B **36**, 6712 (1987).
23. D. Auvergne, J. Camassel, and H. Mathieu, Phys. Rev. B **11**, 2251 (1975).
24. T. Huo, L. Yan, J. Si, *et al.*, J. Mater. Chem. C **11**, 3736 (2023).
25. C. Wang, L. Yan, J. Si, *et al.*, J. Alloys Compd. **946**, 169272 (2023).
26. J. Sung, C. Schnedermann, L. Ni, *et al.*, Nat. Phys. **16**, 171 (2020).